In Situ Precipitation of Silica in Dansyl-Labeled Poly(dimethylsiloxane) Elastomers

Pieter B. Leezenberg† and Curtis W. Frank*,‡

Departments of Materials and Science and Engineering and Chemical Engineering, Stanford University, Stanford, California 94305-5025

Received October 21, 1994. Revised Manuscript Received July 26, 1995®

Silica was precipitated in situ within end-linked poly(dimethylsiloxane) (PDMS) networks using a variety of acidic and basic catalyst solutions. The resulting silica loading level varied between 20 and 35 wt %. The PDMS networks had the 1-(dimethylamine)-5-naphthalenesulfonyl (dansyl) chromophore covalently attached to the cross-link junctions. We used dansyl steady-state fluorescence to probe the rigidity of the local environment around the cross-links. An emission band indicating limited mobility is attributed to the presence of a layer of adsorbed network polymer near a hydrophilic silica interface. In the absence of such an emission band, we conclude that the interface is hydrophobic. Using small-angle X-ray scattering, we determined the structure of the silica phase. Basic catalysts gave discrete silica particles, while acidic catalysts resulted in interpenetrating networks of silica and siloxane polymer. These structural features are correlated with the swelling behavior of the nanocomposites: the basic catalysts result in stronger reinforcement than the acid catalysts. The interface chemistry has only a subordinate effect on the modulus.

Introduction

For most practical applications, PDMS elastomers are reinforced with some filling material. These fillers can be introduced in a variety of ways. Recently, the in situ precipitation of silica and other inorganic phases in different polymer matrices has been reported.[1–8] This technique employs methods from sol–gel chemistry to precipitate the inorganic phase from alkoxy compounds inside a polymer matrix at room temperature, in the presence of a catalyst. This approach allows direct control over the molecular structure of the resulting composite materials, which are therefore called molecular or nanocomposites.

The magnitude of the reinforcing effect is dependent on the structure and dispersion of the silica phase. One important factor that determines the structure of the inorganic phase is the pH of the catalyst solution, since the relative rates of hydrolysis and condensation change with pH.[6] It has been reported that high-pH catalyst solutions result in discrete spherical silica particles, whereas low-pH solutions result in network-like silica structures interpenetrating the polymer matrix.[3,4,6,9–11] The structure of these composite materials has been investigated using dielectric spectroscopy,[7,8] electron microscopy,[4] small-angle X-ray scattering (SAXS),[5,6,11–13] XPS,[13] ^{29}Si NMR,[14] and dynamic mechanical spectroscopy. The increase in modulus in silica–siloxane nanocomposites that is associated with the introduction of the silica phase is not clearly correlated with the observed morphology of this phase. The interaction mechanisms between silica and siloxane that are thought to be responsible for reinforcement effects on the modulus are discussed elsewhere.[15]

The molecular origin of the reinforcing effect of the silica in these materials is not completely understood.[16–18] Mixtures of silica particles and PDMS have been studied using ^{2}H NMR[19,20] and dielectric spectroscopy.[21] The dynamics of the polymer segments are strongly dependent on the surface activity of the silica. If the surface of the silica is hydrophilic, an adsorption layer exists

† Department of Materials Science and Engineering.
‡ Department of Chemical Engineering.
* To whom correspondence should be addressed.
® Abstract published in *Advance ACS Abstracts,* September 1, 1995.

(1) Novak, B. M. *Adv. Mater.* **1993**, *5*, 422.
(2) Jiang, C.-Y.; Mark, J. E. *Makromol. Chem.* **1984**, *185*, 2609.
(3) Mark, J. E.; Schaefer, D. W. In *Polymer Based Composites*; Schaefer, D. W., Mark, J. E., Eds.; Materials Research Society: Pittsburgh, 1990; Vol. 171, p 51.
(4) Ning, Y.-P.; Mark, J. E. *Polym. Bull.* **1984**, *12*, 407.
(5) Schaefer, D. W.; Mark, J. E.; McCarthy, D.; Jian, L.; Sun, C.-C.; Farago, B. In *Polymer Based Composites*; Schaefer, D. W., Mark, J. E., Eds.; Materials Research Society: Pittsburgh, 1990; Vol. 171, p 57.
(6) Wilkes, G. L.; Huang, H, H,; Glaser, R. H. In *Silicon-Based Polymer Science, A Comprehensive Resource*; Zeigler, J. M., Fearon, F. W. G., Eds.; American Chemical Society: Washington, DC, 1990; Vol. 224, p 207.
(7) Landry, C. J.; Coltrain, B. K.; Brady, B. K. *Polymer* **1992**, *33*, 1486.
(8) Landry, C. J.; Coltrain, B. K.; Wesson, J. A.; Zumbulyades, N.; Lippert, J. L. *Polymer* **1992**, *33*, 1496.
(9) Mark, J. E.; Ning, Y.-P. *Polym. Bull.* **1984**, *12*, 413.
(10) Ning, Y.-P.; Mark, J. E. *Polym. Eng. Sci.* **1986**, *26*, 167.
(11) Schaefer, D. W.; Mark, J. E.; Sun, C.-C.; McCarthy, D. W.; Jiang, C.-Y.; Ning, Y.-P.; Spooner, S. In *Ultrastructure Processing of Advanced Materials*; Uhlmann, D. R., Ulrich, D. R., Eds.; John Wiley & Sons: New York, 1992.
(12) Xu, P.; Wang, S.; Mark, J. E. In *Better Ceramics Through Chemistry IV*; Zelinski, B. J. J., Brinker, C. J., Clark, D. E., Ulrich, D. R., Eds.; Materials Research Society: Pittsburgh, 1990; Vol. 180, p 446.
(13) Nandi, M.; Conklin, J. A.; Salvati, L.; Sen, A. *Chem. Mater.* **1991**, *3*, 201.
(14) Iwamoto, T.; Morita, K.; Mackenzie, J. D. *J. Non. Cryst. Solids* **1993**, *159*, 65.
(15) Leezenberg, P. B. Ph.D. Thesis, Stanford University, 1994.
(16) Eichinger, B. E. *Annu. Rev. Phys. Chem.* **1983**, *34*, 359.
(17) Kloczkowski, A.; Sharaf, M. A.; Mark, J. E. In *PMSE*; ACS: Washington, DC, 1993; p 203.
(18) Witten, T. A.; Rubinstein, M.; Colby, R. H. *J Phys. II France* **1993**, *3*, 367.
(19) Litvinov, V. M.; Spiess, H. W. *Makromol. Chem.* **1992**, *193*, 1184.
(20) Litvinov, V. M.; Spiess, H. W. *Makromol. Chem.* **1991**, *192*, 3005.
(21) Kirst, K. U.; Kremer, F.; Litvinov, V. M. *Macromolecules* **1993**, *26*, 975.

0897-4756/95/2807-1784$09.00/0

around the silica particle that is between 10 and 20 Å thick. Even above T_g, the motions of the chain segments are severely limited in this boundary region, whereas outside this region they are mobile. Besides restricted polymer segmental motion, slow adsorption and desorption processes occur in the 10–20 Å thick boundary layer. If the surface is hydrophobic, there is no evidence of a strongly bound polymer layer.

Experimental work on the molecular structure using optical probe molecules has been done on different molecular composites[22,23] and sol–gel materials.[24–28] Changes in the matrix surrounding the probe molecule were monitored on a length scale of several angstrom. However, these probes were randomly dispersed in the material and do not give site–specific information.

The purpose of the present study is to investigate the local structure of in situ formed molecular composites, specifically in the environment of the cross-links. To this end we observe steady-state fluorescence emission of the fluorescent molecule 1-(dimethylamino)-5-naphthalenesulfonyl (dansyl) covalently bound to cross-link junctions inside molecular composites. The maximum fluorescence emission energy of dansyl is strongly dependent on the polarity of its local environment. Because of this solvatochromic behavior, dansyl has been used to probe the microenvironment in synthetic polymer systems,[29–34] self-organizing systems,[35] and surfaces.[36–38]

We prepare fluorescent model networks by end-linking silanol-terminated PDMS with a mixture of trifunctional alkoxysilanes and record the emission spectrum. Subsequently, we let silica precipitate in situ. Changes of the fluorescence emission properties after precipitation of silica indicate modifications occurring in the local environment of the labeled cross-link junctions.

In the following we report the effects of fluorescence emission of a number of variables that affect the structure of the molecular composite. These variables include the type of catalyst used in preparing the samples, the time that the samples were immersed in the catalyst solution, the type of precipitating reagent and swelling of the composites in different solvents. We interpret the resulting fluorescence spectra in terms of the local structure around the cross-link junctions.

Experimental Section

For network preparation hydroxyl-terminated PDMS (750 cs), *N*-(triethoxysilylpropyl)dansylamide (DTES), methyltriethoxysilane (MTES) and tin octoate were all obtained from Hüls-Petrarch and were used without further purification. Through GPC, we found the number-average molecular weight of the PDMS to be 15 000 with a polydispersity index of 1.98. The PDMS was end-linked at room temperature using a mixture of trifunctional ethoxysilanes with a stoichiometric ratio of two ethoxy groups per chain end. A cross-linker mixture was prepared containing 99.9 mol % MTES and 0.1 mol % DTES, diluted in 40 vol % THF. This mixture was pipetted into PDMS and stirred. Then 1 wt % catalyst (50% catalyst dissolved in methyl-terminated PDMS) was added and stirred for 3 min. Polyethylene-embedding molds were filled with 2.5 mL of the uncured mixture. These samples were cured at room temperature under nitrogen for 48 h at a relative humidity of 15%, followed by 72 h under vacuum. The samples were then swollen in THF for 72 h to extract all unreacted materials. Next, increasing amounts of methanol were added to deswell the samples. The weight fraction of extracted materials was gravimetrically determined as $w_s = 0.07 \pm 0.005$. All weighing was done on a Mettler A240 microbalance with an accuracy of 10^{-4} g.

Extracted network samples were weighed and then swollen in tetraethoxysilane (TEOS). In equilibrium, v_{2m}, the volume fraction of polymer in the swollen network, was 0.29. TEOS was obtained from Fisher Scientific and vacuum distilled prior to use. The swollen networks were placed in different acidic or basic aqueous solutions prepared from Millipore water for 1 or 2 h. Subsequently, we dried the samples in air, after which we extracted them for 7 days in THF that was periodically renewed. The samples were deswelled by adding increasing fractions of methanol to the THF. Finally, the samples were dried in air for 48 h and in vacuum for 48 h.

We also prepared a set of samples with the precipitation product of methyltriethoxysilane (MTES) inside. We followed the same protocol as described above but used trifunctional MTES instead of tetrafunctional TEOS for precipitation. In MTES, v_{2m} of the swollen network is 0.19.

We extracted the filled samples extensively to remove residual silanes, acid, base, or counterions from the samples, since the dansyl quantum yield is strongly pH dependent.[36] However, differences in emission spectra prior to and after extraction were negligible.

The pH of the aqueous catalyst solutions was determined using a Beckman Φ44 pH meter. The following bases and acids (with the pH of the solution indicated in parentheses) were used to precipitate silica in separate networks: triethylamine (12.3), ethylamine (12.1), tetramethylammonium hydroxide (TMAH) (11.7), formic acid (2.4), glacial acetic acid (2.3), and oxalic acid dihydrate (2.1).

Steady-state fluorescence spectra were measured with a Spex Fluorolog 212 spectrometer with a 450 W xenon lamp. We used slit widths of 2 mm, corresponding to spectral bandwidths of 5 nm. All spectra were measured against a reference solution of rhodamine B in propylene glycol and were corrected for nonlinearities. The sample holder for swollen networks is described elsewhere.[30]

SAXS experiments were done at the Stanford Synchrotron Radiation Laboratory. The detector was a EG&G/PAR X-ray photodiode with 25 μm pixel size. The setup contained a Si (111) curved monochromator with an energy resolution $\Delta E/E = 4 \times 10^{-3}$ at 8.67 keV. The energy we used for our experiments was 8.3 keV, corresponding to $\lambda = 1.495$ Å.

Filling PDMS networks with an inorganic phase greatly increases the amount of light scattering. To see if the fluorescence spectra were modified as a result of this scattering, we performed emission spectroscopy on two composite samples without dansyl. These samples were prepared using

(22) Hanna, S. D.; Dunn, B.; Zink, J. I. *J. Non. Cryst. Solids* **1994**, *167*, 239.
(23) Jeng, R. J.; Chen, Y. M.; Jain, A. K.; Kumar, J.; Tripathy, S. K. *Chem. Mater.* **1992**, *4*, 1141.
(24) Narang, U.; Jordan, J. D.; Bright, F. V.; Prasad, P. N. *J. Phys. Chem.* **1994**, *98*, 8101.
(25) Fujii, t.; Kitamura, H.; Kawauchi, O.; Mabuchi, T.; Negishi, N. *J. Photochem. Photobiol. A* **1991**, *61*, 365.
(26) Lebeau, B.; Herlet, N.; Livage, J.; Sanchez, C. *Chem. Phys. Lett.* **1993**, *206*, 15.
(27) Matsui, K.; Tominaga, M.; Arai, Y.; Satoh, H.; Kyoto, M. *J. Non. Cryst. Solids* **1994**, *169*, 295.
(28) Severin-Vantilt, M. M. E.; Oomen, E. W. J. L. *J. Non. Cryst. Solids* **1993**, *159*, 38.
(29) Yamanaka, T.; Takahashi, Y.; Uchida, K. *Chem. Phys. Lett.* **1990**, *172*, 405.
(30) Hoffmann, D. A.; Anderson, J. E.; Frank, C. W. *J. Mater. Chem.*, in press.
(31) Hu, Y.; Horie, K.; Ushiki, H. *Macromolecules* **1992**, *25*, 6040.
(32) Hu, Y.; Horie, K.; Ushiki, H.; Tsunomori, F.; Yamashita, T. *Macromolecules* **1992**, *25*, 7324.
(33) Leezenberg, P. B.; Frank, C. W. *Macromolecules*, submitted.
(34) Shea, K. J.; Stoddard, G. J. *Macromolecules* **1991**, *24*, 1207.
(35) Shea, K. J.; Stoddard, G. J.; Shavelle, D. M.; Wakui, F.; Choate, R. M. *Macromolecules* **1990**, *23*, 4497.
(36) Seo, T.; Take, S.; Miwa, K.; Hamada, K.; Iijima, T. *Macromolecules* **1991**, *24*, 4255.
(37) Holmes-Farley, S. R.; Whitesides, G. M. *Langmuir* **1986**, *2*, 266.
(38) Lochmuller, C. H.; Marshall, D. B.; Wilder, D. R. *Anal. Chim. Acta* **1981**, *130*, 31.

Table 1. Composition and Swelling Properties of the Molecular Composite Samples[a]

catalyst	time (h)	precipitant	w_{in}	w_2 in THF	w_2 in MeOH
unfilled			0.000	0.160	0.962
ethylamine	1	TEOS	0.244	0.470	
ethylamine	2	TEOS	0.303	0.493	0.972
ethylamine	2	MTES	0.185	0.233	
triethylamine	2	TEOS	0.280	0.488	
TMAH	2	TEOS	0.266	0.475	
acetic acid	1	TEOS	0.187	0.233	
acetic acid	2	TEOS	0.249	0.274	0.964
acetic acid	24	TEOS	0.302	0.346	
acetic acid	2	MTES	0.215	0.245	
oxalic acid	2	TEOS	0.348	0.265	
formic acid	2	TEOS	0.278	0.249	

[a] Catalyst, time of immersion, and precipitant used in preparation of molecular composite; resulting w_{in}, weight fraction of inorganic phase precipitated inside PDMS elastomer, and w_2, weight fraction of (polymer and silica) phase inside composites swollen to equilibrium in methanol or tetrahydrofuran.

acetic acid and ethylamine in the same way as described above, but they were end-linked without DTES. We did not see any emission bands from these samples above the background noise in the relevant wavelength range. However, one effect related to scattering is that we cannot compare intensities from different samples, since the amount of scatter varies strongly with the structure and volume fraction of the scattering phase.

We performed DSC measurements with a DuPont Thermal Analyst 2100 on an unfilled sample and on the samples prepared with acetic acid, formic acid, oxalic acid, and ethylamine. We scanned from 123 to 293 K after an initial cooling run, using liquid nitrogen.

To obtain fluorescence spectra at low temperature, we used a cryogenic microminiature refrigeration system IIB, Model K 2205, by MMR Technologies. This Joule–Thomson system operates with 1800 psi of nitrogen. The automated temperature control indicated that the temperature at 80 K was stable to ±0.1 K.

Results

Equilibrium Swelling in Tetrahydrofuran. The weight fraction of silica precipitated inside the network is dependent on the type of the catalyst present. In Table 1, we show w_{in}, the weight fraction of silica that results from precipitation using six different catalysts in aqueous solution for various immersion times and precipitants. As a result of these different processing conditions, the properties of the materials change considerably.

For all samples, we determined w_2, the weight fraction of (polymer and silica) phase inside composites swollen to equilibrium in tetrahydrofuran. In unfilled networks we see a small w_2, corresponding to a large degree of swelling. In all of the filled networks, the degree of swelling is considerably smaller. Increasing the immersion time in a given catalyst solution increases w_{in}, the silica loading level, and correspondingly decreases the amount of swelling. The basic catalysts yield composites that have roughly the same silica loading level as the composites formed with acid catalysts, but they swell considerably less than those prepared with the acid catalysts. For the limited set of catalysts and pH values that we used, the reinforcing effect is correlated with pH rather than with the nature of the catalyst in solution.

Steady-State Fluorescence. The fluorescence emission energy of dansyl depends strongly on the polarity and the cohesion of the surrounding medium.[39-42] In general, the solvatochromic effect is caused by relaxation of the solvent dipoles during the excited-state lifetime. The energy of the stable emitting state depends on the strength of the dipoles surrounding the probe during its excited-state lifetime. The dimethylamino group donates an electron into the excited π^*-system of the naphthalene. Mixing of the excited state and this charge-transfer state depends on the polarity of the local environment of the probe.[40]

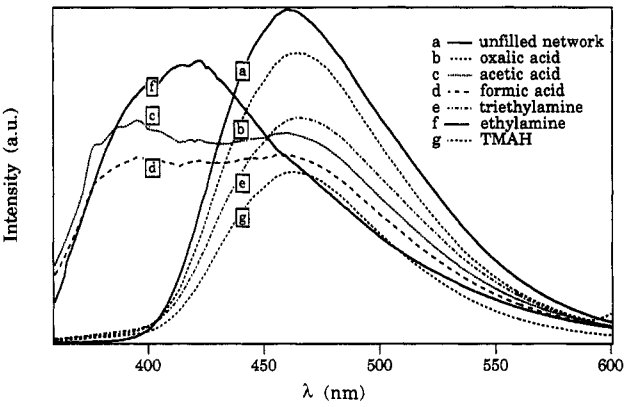

Figure 1. Fluorescence emission spectra of PDMS networks in which silica has been precipitated from TEOS, using different catalyst solutions for 2 h; excited at λ_{exc} = 340 nm.

Dansyl emission is related to the rigidity of the medium as well. In a range of solvents, the emission energy from dansyl-like compounds was more strongly correlated with the solubility parameter than with the dielectric constant.[42] In mobile media, the solvation shell surrounding a dansyl relaxes rapidly and emission occurs from the excited state with the lowest energy. When the surrounding medium is rigid, the solvating dipoles do not relax around the excited state. The energy of the charge-transfer state is dependent on the angle between the dimethylamino and the naphthalene system. When the rearrangement of the dimethylamino group is hindered, relaxation cannot occur, and fluorescence emission occurs from a high-energy excited state.

In Figure 1 we plot the emission spectra of six networks filled with silica, employing different catalyst solutions for 2 h, obtained with an excitation wavelength, λ_{exc}, of 340 nm. The shapes of the spectra obtained from these samples are strongly correlated with the nature of the catalyst solution. For reference we also show the emission spectrum from the unfilled network. The intensity from these samples varies strongly; to put the spectra all in the same graph, we have adjusted the relative scale.

At room temperature, the emission spectrum of the dansyl-labeled PDMS elastomer without the reinforcing phase shows a single band with a band width of approximately 3800 cm^{-1} and an emission maximum around 21 700 cm^{-1}.

(39) Lochmuller, C. H.; Marshall, D. B.; Harris, J. M. *Anal. Chim. Acta* **1981**, *131*, 263.
(40) Ghiggino, K. P.; Lee, A. G.; Meech, S. R.; O'Connor, D. V.; Phillips, D. *Biochemistry* **1981**, *20*, 5381.
(41) Li, Y.-H.; Chan, L.-M.; Tyer, L.; Moody, R. T.; Himel, C. M.; Hercules, D. M. *J. Am. Chem. Soc.* **1975**, *97*, 3118.
(42) Meech, S. R.; O'Connor, D. V.; Phillips, D. *J. Chem. Soc., Faraday Trans. 2* **1983**, *79*, 1563.

From the sample prepared with oxalic acid, we obtain a spectrum with an emission band almost identical to the unfilled network. From the samples prepared with acetic acid or formic acid, we obtain emission spectra with multiple peaks. Since the pH of all the acidic solutions was approximately the same, the dansyl fluorescence strongly depends on the nature of the acid.

Emission from samples prepared with triethylamine or TMAH is similar to emission from the unfilled network. Emission from the samples prepared with ethylamine also shows a single broad band, but it is broader and substantially blue-shifted relative to the triethylamine or TMAH samples. Again, the pH of the basic catalyst solutions was the same, so the dansyl emission is correlated with the nature of the catalyst, rather than with the pH.

The presence of broad bands or multiple peaks at these energies has, to our knowledge, not been observed before in dansyl fluorescence. It suggests that multiple populations of the dansyl species exist, and these are emitting at different wavelengths. Different moieties within the same sample experience different local environments, leading to a range of emitting states and hence to a range of emission energies. If part of the dansyl population remains unaffected by the presence of the silica, then we can now see how the rest of the dansyl population is affected by subtracting the normalized emission of the unfilled network from the emission spectrum that we obtain from these nanocomposites.

We show the results of this spectral subtraction in Figure 2A for ethylamine and in Figure 2B for formic acid. After subtraction, in these samples a single, well-defined emission band appears at energies that are uncharacteristically high for dansyl. A single narrow band results, with maximum emission energies around $\lambda = 395$ nm for samples prepared with formic and acetic acid. For the ethylamine sample, a band results with maximum emission energy around $\lambda = 405$ nm. The effect of precipitating silica appears to subject the dansyl population to two different environments in these samples. The high-energy band in the ethylamine sample is red-shifted 10 nm relative to the high energy band in the two acid samples.

Differential Scanning Calorimetry. In the unfilled network we found a glass transition (T_g) at 148 K and a melting transition (T_m) at 233 K. In Table 2 we report these observations as well as the T_g and T_m of networks in which we precipitated silica with ethylamine, acetic acid, formic acid and oxalic acid for 2 h.

Precipitation of silica does not affect the T_g, but it does cause a melting point depression. This suggests that crystallization of PDMS is hindered by the presence of silica.[43] The melting point depression is weakly correlated with the weight fraction of silica. The effect is the strongest in the ethylamine sample.

Red-Edge Effect. In a mobile medium, the emission is independent of the excitation wavelength, λ_{exc}, due to rapid relaxation of the medium dipoles. In a rigid medium, however, the solvent cage relaxes relatively slowly and emission occurs from excited states with various energies. The maximum emission energy is dependent on the excitation wavelength, λ_{exc} at the red edge of the absorption band. This is called the red-edge effect.[38,44,45]

We looked for a possible red-edge effect in all our samples to obtain information about the local rigidity of the cross-link environment. In the unfilled networks and in samples containing silica precipitated with oxalic acid, triethylamine, or TMAH we see no red-edge effect; the position of the emission band is independent of λ_{exc}. On the other hand, we see a strong dependence of the emission on λ_{exc} in the composite samples prepared with ethylamine, acetic acid and formic acid. In Figure 3A,B, we show the emission spectra at three different excita-

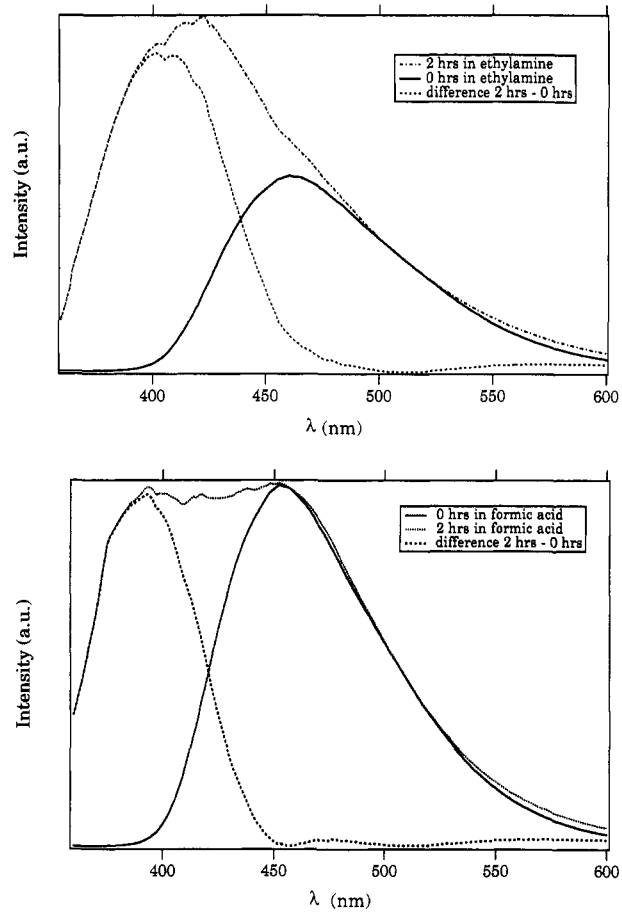

Figure 2. (a, top) Fluorescence emission spectra ($\lambda_{exc} = 340$ nm, normalized) of a composite prepared using ethylamine, a PDMS network and a difference spectrum between these two. (b, bottom) Fluorescence emission spectra ($\lambda_{exc} = 340$ nm, normalized at $\lambda = 460$ nm) of a composite prepared using formic acid for 2 h, a PDMS network and a difference spectrum between these two.

Table 2: Thermal Properties of Selected Molecular Composites[a]

catalyst	w_{in}	T_g (K)	T_m (K)
(unfilled)	0.000	148	233
ethylamine	0.303	149	225
acetic acid	0.249	148	229
oxalic acid	0.348	149	227
formic acid	0.278	147	230

[a] Catalyst used for 2 h to precipitate silica from TEOS; w_{in}, weight fraction of silica precipitated inside PDMS elastomer; T_g and T_m, glass and melting transition temperatures, respectively.

(43) Reeves, R. L.; Maggio, M. S.; Costa, L. F. *J. Am. Chem. Soc.* **1974**, *96*, 5917.

(44) Clarson, S. J.; Mark, J. E.; Dodgson, K. *Poly. Commun.* **1988**, *29*, 208.

(45) Demchenko, A. P.; Sytnik, A. I. *Proc. Natl. Acad. Sci. U.S.A.* **1991**, *88*, 9311.

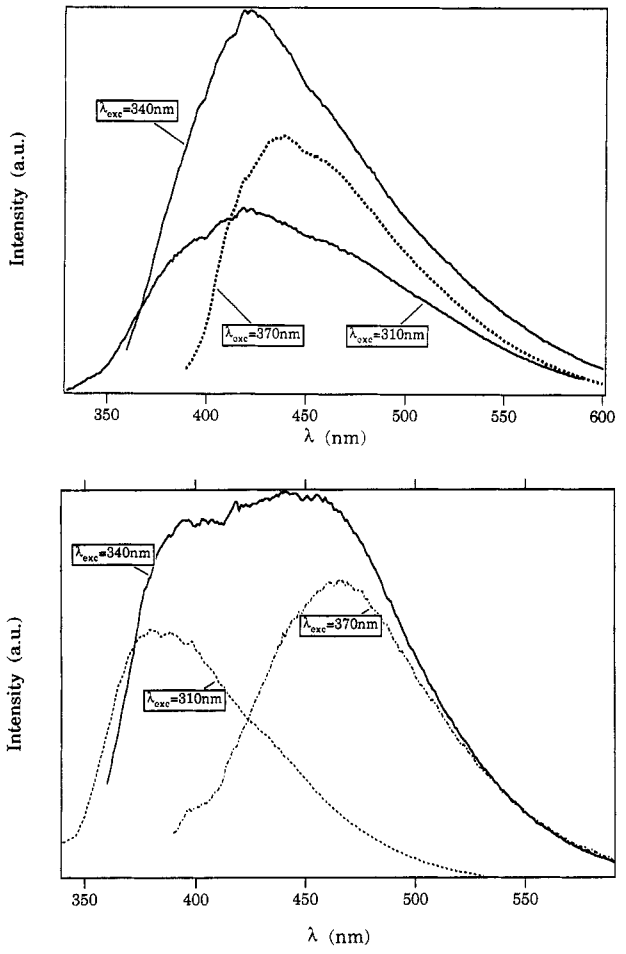

Figure 3. (a, top) Fluorescence emission spectra of an ethylamine composite excited at three different wavelengths: λ_{exc} = 310, 340 and 370 nm. (b, bottom) Fluorescence emission spectra of an acetic acid composite excited at three different wavelengths: λ_{exc} = 310, 340, and 370 nm.

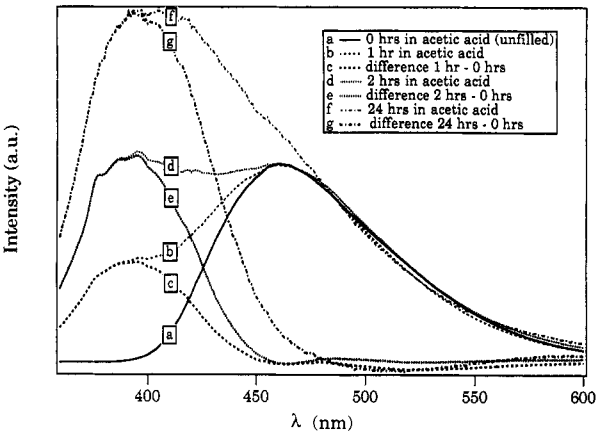

Figure 4. Effect of silica growth on fluorescence emission spectra: composites prepared using acetic acid for different immersion times.

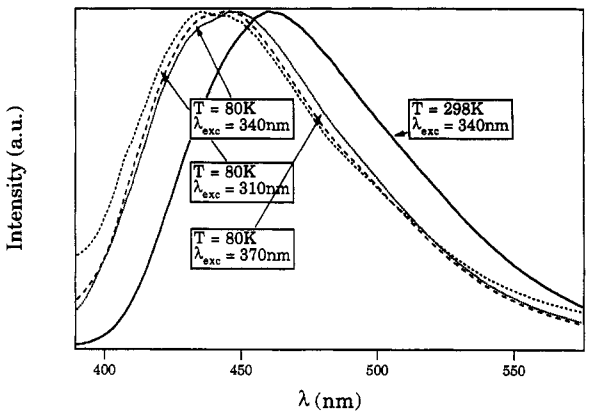

Figure 5. Fluorescence emission spectra of a PDMS network at 298 K (λ_{exc} = 340 nm) and at 80 K, at three different excitation wavelengths: λ_{exc} = 310, 340, and 370 nm.

tion wavelengths from samples prepared with ethylamine and acetic acid, respectively.

In the ethylamine samples in Figure 3A, we see a wide band with a peak around 420 nm when we excite at λ_{exc} = 310 nm and a slightly narrower band with a maximum around 435 nm when λ_{exc} = 370 nm. These band positions are close to each other relative to the acid samples, where the red-edge effect is stronger.

When we excite the acetic acid samples at λ_{exc} = 370 nm, we obtain fluorescence from a dansyl population that is similar to the unfilled network. Exciting at λ_{exc} = 310 nm, we see fluorescence in Figure 3B with a high-energy peak around 400 nm. When λ_{exc} = 340 nm, we see the same wide band as shown in Figure 1. The observed red-edge effect is the same in the formic acid sample.

In the ethylamine, acetic acid and formic acid samples, we see a definite red-edge effect, which we attribute to a rigid local environment of the dansyls. In the other samples we see no red-edge effect. The local rigidity that the dansyls probe is dependent on the nature of the catalyst.

Time of Immersion in Catalyst Solution. The longer the samples are in contact with the catalyst solution, the higher the weight fraction of silica, as shown in Table 1. In Figure 4 we show the change of the dansyl emission spectrum from samples that have been exposed to 2% acetic acid solutions for 1, 2, and 24 h. We normalized the intensity to make the red side of the observed emission bands overlap. We observe similar effects in samples prepared with formic acid for 1 or 2 h. On the other hand, on this time scale there is no dependence of the fluorescence on the time of exposure in the samples prepared with ethylamine.

In Figure 4 we also show the difference between the acetic acid nanocomposite emission spectra and the unfilled network spectrum, similar to Figure 2B. The intensity of the high-energy band increases relative to the emission band around 460 nm with time of immersion and is therefore positively correlated with the weight fraction of silica. This indicates that an increasing part of the dansyl population is submitted to mobility constraints by a rigid environment. However, there is no change in the position of the high-energy band with increasing loading level of silica. The local rigidity does not change any further; only the distribution of the dansyl population between the rigid and the mobile fractions of the composite changes.

Low-Temperature Fluorescence. As a reference experiment, we have measured the fluorescence emission spectrum of an unfilled dansyl-labeled network at 80 K, well below T_g. We show the emission spectra in Figure 5 for λ_{exc} = 310, 340, and 370 nm, respectively. At this temperature both a blue-shift and a slight red-edge effect are visible, compared to Figure 3. This confirms that the local environment of the labeled cross-links is slightly more rigid in the frozen network than above T_g.

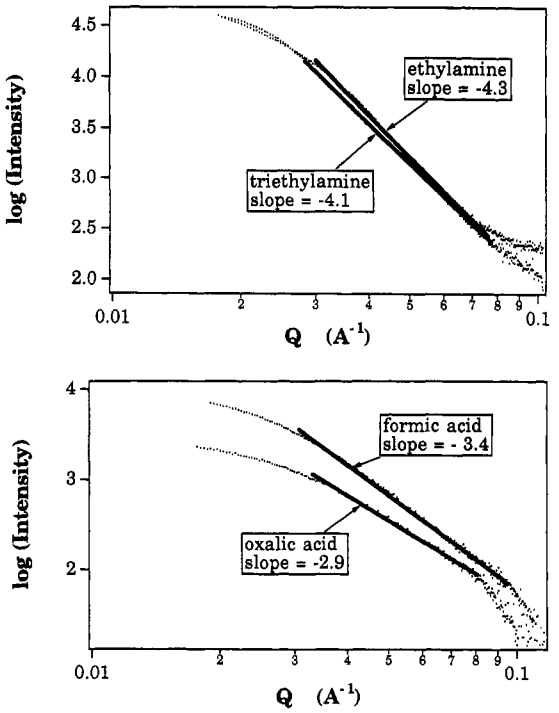

Figure 6. (a, top) Small-angle X-ray spectra of composites prepared using ethylamine and triethylamine for 2 h. (b, bottom) Small-angle X-ray spectra of composites prepared using acetic acid and formic acid for 2 h.

In addition, it has been reported that fluorescence of dansyl dissolved in 1-butanol blue-shifts as the temperature decreases and the viscosity of the medium increases,[39] resulting in an emission band with a peak at 435 nm at 85 K.

When we compare these results to the residual high-energy bands in Figure 2A,B, the low-temperature band position is at a relatively low energy. This suggests that a portion of the dansyls inside the polymer/silica composite probe a local mobility that is lower than in either PDMS or 1-butanol, which has been cooled to below T_g.

Small-Angle X-ray Scattering. In small-angle X-ray scattering (SAXS) experiments we measured the angular dependence of the scattered intensity, I, when the sample was irradiated with X-rays. The intensity of the scattered X-rays is expressed as a function of the wave vector $Q = (2\pi/\lambda)\sin(\theta/2)$. The scattered intensity has a power-law dependence on Q. In the relevant Q range, the slope of the $\log(I)$ vs $\log(Q)$ plot is called the Porod slope and contains information about the fractal nature of the silica phase.[5,11,46,47]

In Figure 6A we show the $\log(I)$ vs $\log(Q)$ diagrams for samples catalyzed by ethylamine and triethylamine. In Figure 6B we plot the same for formic acid- and oxalic acid-catalyzed samples. In both figures, we include a fitted line in the Porod region.

The Porod slope for the base-catalyzed samples in Figure 6A is -4.2 ± 0.1. This suggests a uniformly dense silica phase, organized in discrete particles, with smooth surfaces.[46] It has previously been found[11] that particles grown in situ under similar conditions in 25% aqueous ethylamine solution are compact and have a mean cluster radius of approximately 100 Å. The Porod slope for the acetic acid-catalyzed sample is -3.0. For the acid-catalyzed samples in general we find a Porod slope of -3.1 ± 0.3, indicating that the silica forms a dense polymer or a rough colloid.[11,46] This fractal structure forms an interpenetrating network with the PDMS.

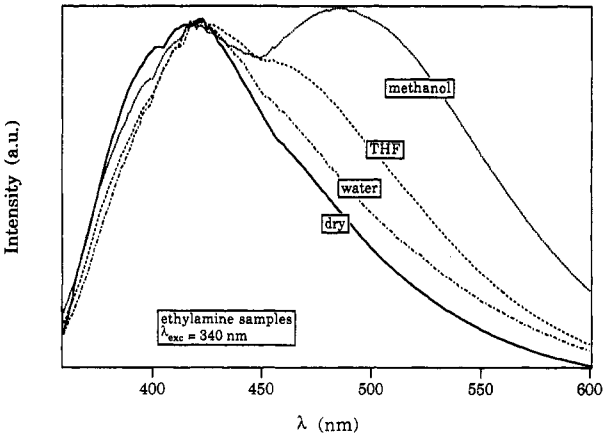

Figure 7. Fluorescence emission spectra of ethylamine composite dry and swollen in water, methanol, or tetrahydrofuran (λ_{exc} = 340 nm).

Under basic conditions, hydrolysis is slow relative to condensation and nucleation, and reaction-limited aggregation processes lead to nonfractal colloidal particles. Using an acid catalyst, condensation is slow relative to hydrolysis and reaction-limited cluster aggregation leads to polymeric fractal structures.[41] We find that the Porod slope and therefore the fractal nature of the silica is dependent only on the pH of the catalyst solution. Our experiments indicate that there is no correlation between the type of catalyst used and the fractal dimensions of the silica, provided that a uniform synthetic protocol is used for the in situ precipitation.

Fluorescence from Swollen Networks. An additional way to probe the composite structure around the dansyl moieties is to determine how accessible these moieties are to solvent molecules. Introducing polar solvent molecules into the solvation shell of the dansyl is expected to red shift the emission spectrum. Previously, it has been found that filling a rubber with particulate silica reduces the amount of solvent taken up in swelling equilibrium.[48] It was suggested that the polymer is less readily solvated due to reduced mobility when segments are adsorbed at the silica surface.

We placed composite samples in excess amounts of water, methanol, and tetrahydrofuran (THF), respectively. The equilibrium amount of water that is taken up is approximately 0.1 wt %. In equilibrium, the other two solvents swell the composites to the extent shown in the last two columns in Table 1.

From swollen unfilled network samples, we obtain emission spectra with a single band.[32] The band maximum is at 465 nm when the elastomer is swollen in water, 510 nm in methanol, and 500 nm in THF.

In Figure 7, we plot the emission spectra for the ethylamine samples, both dry and swollen, normalized at 415 nm. Swelling the composite with water red shifts the emission band slightly compared to the dry sample. The low-energy band becomes relatively more intense when methanol or THF swells the composites. The

(46) Valeur, B.; Weber, G. *J. Chem. Phys.* **1978**, *69*, 2393.
(47) Brinker, C. J.; Scherer, G. W. *Sol-Gel Science*; Academic Press: San Diego, 1990.
(48) Schaefer, D. W. *Science* **1989**, *243*, 1023.

intensity of this band increases when we swell with THF instead of methanol. In addition, the presence of a swelling agent red shifts this low-energy band, whereas the position of the high-energy band remains unchanged.

THF swells the composite materials to a far larger extent than methanol, as can be seen in Table 1. Dilation alone, with subsequent release of some of the "silica-bound" dansyl moieties from their rigid environment, would be expected to cause the low-energy band to be relatively stronger in the THF-swollen composite than in methanol-swollen sample. Since this is not the case, dilation effects are not sufficient to explain the observed red shift.

The introduction of a more polar compound into the dansyl environment can red-shift the emission band disproportionally due to preferential solvation.[32] The low-energy band in the unswollen networks is due to emission by a dansyl population that is interacting only with a mobile environment. Therefore, preferential solvation of these dansyls by the solvent can explain this red shift.

However, a more polar environment usually also decreases dansyl fluorescence intensity.[32] We observe the opposite: an increase in the low-energy band intensity relative to the high-energy band with the introduction of solvent. This leads us to believe that the solvent removes the constraints imposed on a portion of the network-bound dansyls adjacent to the silica. The solvent preferentially wets the silica surface, displacing the polymer and thus increasing the mobility in the adsorbed polymer layer. The fraction of dansyls in the mobile polymer phase increases.

Spatially selective sorption may occur in those samples where the polar surface of the silica causes the polar solvent to sorb preferentially at the silica interface rather than in the polymer-rich regions. H-bonding between water and the interface silanols causes only a small change in the polarity of the interface and hence does not change the structure of the adsorption layer. H-bonding between the polar end of the methanol and the surface silanol enhances the hydrophobicity of the silica surface. This would cause the volume of immobilized adsorbed polymer to decrease and, hence, increase the relative intensity of the low-energy dansyl emission band associated with the mobile network fraction, as is observed.

In Situ Precipitation of MTES. Trifunctional methyltriethoxysilane (MTES) can be used for in situ precipitation of an inorganic phase in the same fashion as tetrafunctional TEOS. A three-dimensional silica structure will be formed inside the labeled PDMS matrix. We wanted to determine the effect on the reinforcement of incorporating hydrophobic methyl in the silica phase. We precipitated this phase from MTES using 2 wt % acetic acid and ethylamine catalyst solutions, resulting in filler loading levels (w_{in}) that are slightly lower than in the case of TEOS; see Table 1. The precipitate formed from MTES results in an increase of the resistance against solvent swelling. This increase is not as large as the increase resulting from precipitation of TEOS, as can be seen in Table 1.

In Figure 8 we plot the emission spectra that we obtained from these samples, along with the spectrum from an unfilled sample, using λ_{exc} = 340 nm. Only a very small red shift is observed upon precipitation of silica from MTES, indicating that the local environment is slightly more polar than in the unfilled network. The identical shapes of the spectra indicate that the polarity of the local environment of the dansyl moieties is identical in both samples.

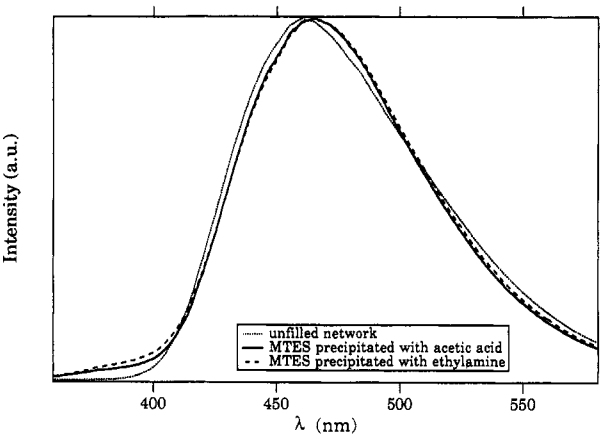

Figure 8. Fluorescence emission spectra of a PDMS network and PDMS networks in which silica has been precipitated from MTES, using ethylamine and acetic acid catalyst solutions for 2 h (λ_{exc} = 340 nm).

We observe no red-edge effect in any of these samples when we vary λ_{exc} from 310 to 370 nm; the bandwidth and band position do not change with λ_{exc}, only its intensity. This is almost identical to what we observed in the unfilled sample. The only difference is a small shoulder occurring at high energy, excited at λ_{exc} = 310 or 340 nm.

Discussion

We can now combine this information about the silica structure as a function of the pH with our fluorescence results, to relate the rigidity of the dansyl environment to the silica morphology.

For the ethylamine, acetic acid, and formic acid, the fluorescence results indicate increased rigidity around part of the dansyl population. There are two possible explanations for this. Either the dansyl-labeled cross-links are incorporated inside the silica phase, or they are immobilized in the adsorption layer surrounding the silica particles. In both environments we expect the local mobility around the dansyl moieties to be severely restricted.

Precipitation of silica from TEOS with ethylamine leads to discrete particles. We see a broad band with a single maximum in this sample, which we deconvolve into two discrete bands in Figure 2A. We conclude that the dansyl moieties experience two types of local rigidity, related to their positioning with respect to the silica particles.

From Figure 6A we infer that the silica particles precipitated at high pH are not fully dense, probably because they grow in an incompatible PDMS matrix.[11] Growing particles must dispose of the incompatible chains and cross-links at the growing interface or incorporate them in their interior. These different processes should result in different local rigidities, with different corresponding effects on the fluorescence of the cross-link bound dansyl moieties.

From Figure 6B we see that with acid catalysts, unlike the case of the ethylamine samples, the silica phase does not have the morphology to completely overgrow a cross-link junction and incorporate it into its interior. This means that the interfacial behavior of the network PDMS near the silica determines the fluorescence emission. From Figure 1 we see that for different acid catalysts, the interfacial behavior of the network polymer is dependent on the nature of the acid.

The samples containing silica precipitated with acetic and formic acid also show a dual emitting population in Figure 2A. These two populations have maxima around 460 and 395 nm. We conclude that these two populations of dansyls experience two distinct environments of different rigidity in the same composite. The silica forms a network-like structure that interpenetrates with the polymer matrix. Some dansyl groups reside in a very rigid environment; some probe a highly mobile, PDMS-rich environment. The local environment related to the high-energy band is slightly more rigid than in the ethylamine sample.

For the acetic acid samples, the time-dependent results in Figure 4 show that the silica grows as the sample is in contact with the catalyst for a longer time and that the high-energy band simultaneously becomes more intense. A growing fraction of the cross-links is captured in the immobile region of a growing volume fraction of silica. However, the rigidity around this immobilized dansyl population apparently does not increase as the volume fraction of silica grows, since the peak position of the high-energy band does not change.

Previously, we observed that little water enters the PDMS network upon swelling in mixed aqueous solvents.[32] In ^{29}Si NMR experiments it has been shown[49] that when oxalic acid is used as a catalyst in nonaqueous sol–gel precipitation from TEOS in ethyl alcohol solution, it forms a silica phase containing very few hydroxyls. If the same were to occur in a PDMS matrix, then the silica surface would be very nonpolar. This would mean that there would be no bound polymer immobilized near the silica interface present in these samples. Hence, the fluorescence signal from dansyl would be independent of the vicinity of the silica phase. This could explain the absence of a high-energy emission peak from dansyl in the oxalic acid system in Figure 1. Analogously, the presence of a nonpolar silica surface may also explain the lack of a high-energy peak in the triethylamine and TMAH samples.

In aqueous solutions of silica particles, complex formation of aromatic compounds on the silica surface has been shown.[50] The documented cases of complexation involve metal cations. Even though neither water nor metal cations are present in our samples after drying, we envisioned a possible interface complex that involved the excited state of the dansyl moieties. To avoid this situation, we extracted all unreacted material extensively, thereby reducing the concentration of the counterions significantly. We argue that the probability of surface complex formation is too small to explain the high-intensity blue-shifted band.

The structure of the silica phase is determined by the presence and concentration of H^+ or OH^- in the reacting system. Although the counterion does not play an active role in the catalysis, its presence apparently determines whether interface silanols are exposed at the interface after silica precipitation. Some catalysts may cause consumption of these silanols in syneresis, when they react with each other to form siloxane Si–O–Si bonds and expel water.[46] This in turn causes the presence or absence of a polymer adsorption layer.

On the basis of the fluorescence emission from the two samples with the inorganic phase precipitated from trifunctional MTES in Figure 8, we conclude that the precipitated filler phase does not increase the local rigidity around the cross-links in either of these samples. The nature of the catalyst has no effect on the mobility of adjacent cross-link junctions. The local structure surrounding the dansyls is unlike the structure created by in situ precipitation of silica from TEOS using the same catalyst. The MTES based filler phase allows substantial motion of the dansyl moieties. The presence of one hydrophobic methyl group per condensed silane on the precipitated phase prevents adsorption of a polymer layer near the interface.

In previous studies,[51,52] the influence of the silica interface chemistry on the composite modulus was experimentally determined. In these studies, particulate silica was mixed in the polymer prior to cure. Treatment of the particulate silica allowed control over the silica interface chemistry. First, through a heat treatment, the hydroxyl population was varied over a range of 2.3–5.3 silanols/nm^2. At these concentrations, the correlation with the mechanical properties of the filled rubber was small. Second, converting the silanols into trimethylsilyl groups through reaction with silane coupling agents caused a drastic change in the reinforcement. As the conversion was changed from 0 to 100%, the modulus dropped by a factor of 5. Another major variable determining the increase in modulus was the silica particle structure.[51] Specifically, the modulus was strongly correlated with silica pore volume.

Composite preparation by mixing prior to cure cannot achieve the silica–siloxane interpenetrating networks that we obtain at low pH. In our study of in situ precipitated silica we observe substantial differences in amount of adsorbed network polymer, depending on the catalyst that we use for precipitation. However, the possible effect that these variations have on equilibrium swelling behavior is dominated by the silica morphology. Topological interactions between the silica and the network polymer are more imporant for reinforcement than adsorption and polymer immobilization near the interface.

Conclusion

We report the use of steady-state fluorescence measurements of the dansyl probe to determine the local

(49) Wagner, M. P. *Rubber Chem. Technol.* **1976**, *49*, 703.
(50) Sugahara, Y.; Sato, S.; Kuroda, K.; Kato, C. *J. Non-Cryst. Solids* **1992**, *147–8*, 24.
(51) *Mineral-Water Interface Geochemistry*; Hochella, M. F., White, A. F., Eds.; Mineral. Soc. Am.: 1990.
(52) Boonstra, B. B.; Cochrane, H.; Dannenberg, E. M. *Rubber Chem. Technol.* **1975**, *48*, 558.
(53) Warrick, E. L.; Pierce, O. R.; Polmanteer, K. E.; Saam, J. C. *Rubber Chem. Technol.* **1979**, *52*, 437.

rigidity inside silica–PDMS nanocomposites. Binding dansyl to the cross-link junctions enables us to obtain information about the rigidity of the local environment around these sites after silica precipitation.

This rigidity is correlated with the nature of the organic catalyst used for silica precipitation. We attribute this to the polarity of the silica interface. Silica with a polar interface has a layer of adsorbed polymer with reduced mobility, which results in a substantial blue-shift of the dansyl fluorescence emission. The local mobility around the dansyl also varies between the different samples containing polar silica. Precipitation of silica with a hydrophobic interface does not result in this blue-shift in the emission spectra.

As the polar silica phase grows, the number of dansyl moieties that are captured in the immobile regions increases. In networks with silica precipitated from MTES, the inorganic structure does not create a rigid environment around the labeled cross-links. We attribute this to the absence of an immobile adsorption region.

Our SAXS results show that the pH of the aqueous catalyst solution is the major factor determining the silica structure, while the nature of the catalyst does not have a significant impact. For the set of catalysts that we selected, changes in the modulus are predominantly associated with the pH of the catalyst solution. The nature of the catalyst at a given pH determines the silica interface chemistry, which has only a secondary effect on swelling behavior. In these samples, the silica interface chemistry determines the rigidity of the polymer adjacent to the silica phase, but the silica morphology determines the magnitude of the reinforcing effect.

Acknowledgment. We would like to acknowledge Professor Alice P. Gast, Eric K. Lin, and Glen A. McConnell for help with performing the SAXS measurements at the Stanford Synchrotron Radiation Laboratory. This work was supported in part by Hitachi Ltd. and in part by Ford Motor Co.

CM9404778